Fractal dimension and b-value mapping in the Andaman-Sumatra subduction zone

Article *in* Natural Hazards · April 2011

DOI: 10.1007/s11069-010-9667-6

CITATIONS
14

READS
455

4 authors:

Sohini Roy
Jadavpur University
1 PUBLICATION **14** CITATIONS
SEE PROFILE

Uma Ghosh
6 PUBLICATIONS **61** CITATIONS
SEE PROFILE

Sugata Hazra
Jadavpur University
166 PUBLICATIONS **1,365** CITATIONS
SEE PROFILE

J. R. Kayal
Retd. Deputy Director General (Head, Geophys), Geol Surv India; CSIR Emeritus Sc…
130 PUBLICATIONS **2,652** CITATIONS
SEE PROFILE

Nat Hazards
DOI 10.1007/s11069-010-9667-6

ORIGINAL PAPER

Fractal dimension and *b*-value mapping in the Andaman-Sumatra subduction zone

Sohini Roy · Uma Ghosh · Sugata Hazra · J. R. Kayal

Received: 23 January 2010 / Accepted: 12 November 2010

Abstract The Andaman-Sumatra subduction zone is seismically one of the most active and complex subduction zones that produced the 26 December 2004 mega thrust earthquake (Mw 9.3) and large number of aftershocks. About 8,000 earthquakes, including more than 3,000 aftershocks ($M \geq 4.5$) of the 2004 earthquake, recorded during the period 1964–2007, are relocated by the EHB method. We have analysed this large data set to map fractal correlation dimension (Dc) and frequency-magnitude relation (*b*-value) characteristics of the seismogenic structures of this ~3,000-km-long mega thrust subduction zone in south-east Asia. The maps revealed the seismic characteristics of the Andaman-Sumatra-Java trenches, West Andaman fault (WAF), Andaman Sea Ridge (ASR), Sumatra and Java fault systems. Prominent N–S to NW–SE to E–W trending fractal dimension contours all along the subduction zone with Dc between 0.6 and 1.4 indicate that the epicentres mostly follow linear features of the major seismogenic structures. Within these major contours, several pockets of close contours with Dc ~ 0.2 to 0.6 are identified as zones of epicentre clusters and are inferred to the fault intersections as well as asperity zones along the fault systems in the fore arc. A spatial variation in the *b*-value (1.2–1.5) is also observed along the subduction zone with several pockets of lower *b*-values (1.2–1.3). The smaller *b*-value zones are corroborated with lower Dc (0.5–0.9), implying a positive correlation. These zones are identified to be the zones of more stress or asperity where rupture nucleation of intermediate to strong magnitude earthquakes occurred.

Keywords Fractal dimension · *b*-value · Subduction zone · Asperity · Epicentres · Active faults

S. Roy (✉) · S. Hazra · J. R. Kayal
School of Oceanographic Studies, Jadavpur University, Kolkata 700032, India
e-mail: sohini.roy54@gmail.com

U. Ghosh
Lalbaba College, Howrah 711202, India

Published online: 07 December 2010

1 Introduction

The earthquake phenomenon has been explained by power-law relations with respect to magnitude, time and space. Fractal is one such power-law relation, which is a two-point spatial correlation function for earthquake epicentres (Kagan and Knopoff 1980; Mandelbrot 1982). It is a sophisticated statistical tool which quantifies the distribution of earthquake epicentres, its randomness and clusterisation (e.g. Ogata 1988; Hirata 1989; Sunmonu and Dimri 1999; Dimri 2000; Teotia and Kumar 2007). It reflects the heterogeneity of seismic activity in a fault system. Another power-law relation is *b*-value, which is a frequency-magnitude relation defined by Gutenberg-Richter (1944). The *b*-value of a region reflects the frequency-magnitude characteristics of seismogenic structures, stress distribution in space and depth (Mogi 1967; Mori and Abercrombi 1997; Wiemer and Wyss 1997; Wiemer et al. 1998; Wyss et al. 2001). It represents a statistical measurement of the relative abundance of large and small earthquakes in a group or cluster. If *b*-value is large, generally large or great earthquakes are relatively rare. There also exists a relationship between the frequency and the length of the faults (Wang and Lu 1997).

The Burmese-Andaman-Sumatra-Sunda arc defines a ~5,500-km-long boundary between the Indo-Australian and Eurasian plates, from Myanmar to Sumatra and Java to Australia (Fitch 1970; Curray et al. 1979). The plate boundary separates the NE-moving Indian plate from the south-east Asian plate that includes Burma, Andaman and Sunda microplates. It has been suggested that the Indian plate converges obliquely towards the Asian plate at an average rate of 54 mm/year (DeMets et al. 1994). The oblique convergence has caused the formation of a sliver plate between the subduction zone and the right-lateral Sumatra and Java fault systems in the southern part and the Sagaing fault system in the northern part and opened the Andaman Sea Ridge (ASR) in the Andaman Sea (Fig. 1). The nature of convergence varies from continental type in the Burmese arc to oceanic type in the Andaman-Sunda arc (Kayal 2008). The Andaman-Sunda arc is seismically very active and falls in the category of highest seismic hazard zone (V) at par with the north-east Indian region with varying degrees of tectonism and volcanic activity along this subducting margin (Curray 2005).

The Andaman-Sumatra section of the subduction zone had produced several large and great earthquakes in the past; some of which generated destructive tsunamis (Bilham 2005). Largest among them are the historical earthquakes that occurred in 1833 ($M \sim 8.7$); 1861 ($M \sim 8.5$); 1881 (Mw 7.9) and 1941 (Mw 7.7) (Fig. 1). While these large earthquakes ruptured only a few hundreds of kilometres (~200 to 300 km) of the plate boundary, the 2004 tsunamigenic Sumatra mega thrust earthquake (Mw 9.3) and its large series of aftershocks ruptured more than 1,300 km length of the arc, stripping the regions that were ruptured in the past as well as the intervening unbroken patches (Bilham 2005) (Fig. 1).

About 8,140 epicentres, including about 3,000 aftershocks of the 2004 earthquake, recorded during the period 1918–2007, are relocated by the EHB method (Engdahl et al. 2007). We have, however, considered about 8,000 relocated EHB events (Fig. 2) that were recorded since the inception of the WWSSN (World Wide Seismograph Station Network). Before 1964, the data set is not complete with respect to magnitude. Magnitude of completeness (threshold magnitude Mo) of the data set for the period 1964–2007 is 4.5. (Fig. 3). We have analysed this large data set to map fractal dimension and *b*-value characteristics of the seismogenic structures of the ~3,000-km-long mega thrust Andaman-Sumatra subduction zone, in the region between 15°S and 15°N latitude and 90°E–125°E longitude. The area is gridded with 2° × 2° spacing with an overlapping of 1°.

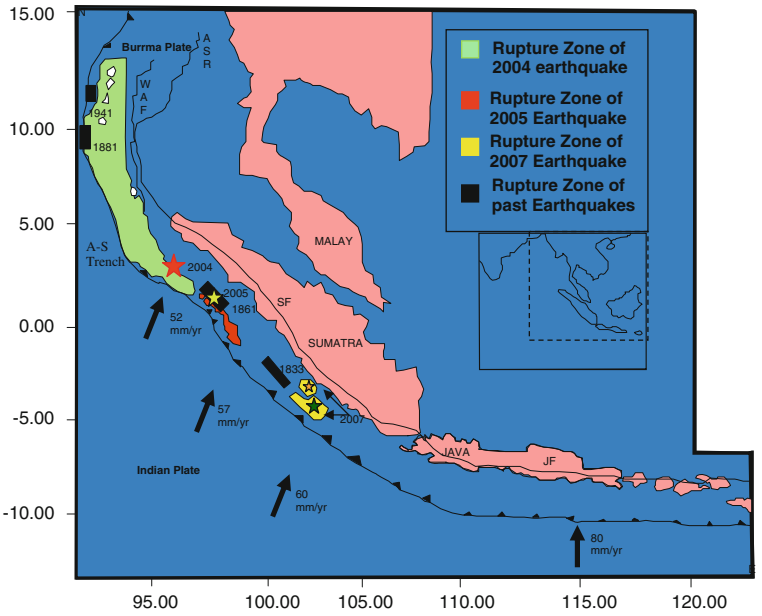

Fig. 1 Tectonic setting of the Andaman-Sumatra Island arc. *WAF* West Andaman Fault, *ASR* Andaman Spreading Ridge, *SFZ* Sumatra Fault Zone, *JFZ* Java Fault Zone, *A-S Trench* Andaman-Sumatra Trench. Plate motions and tectonic features are from Seih and Natawidjaja (2000)

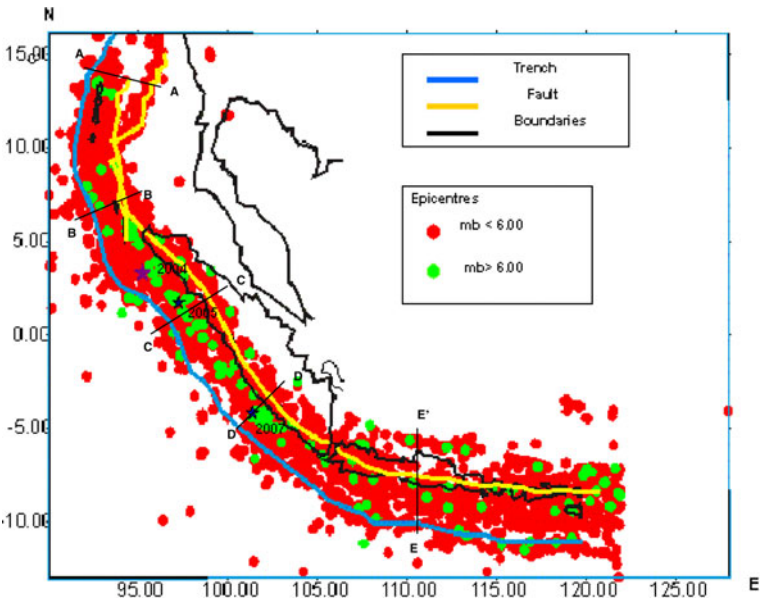

Fig. 2 Epicentre map of about 8,000 (mb > 4.5) earthquakes, relocated EHB data for the period 1964–2007 in the Andaman-Sumatra region

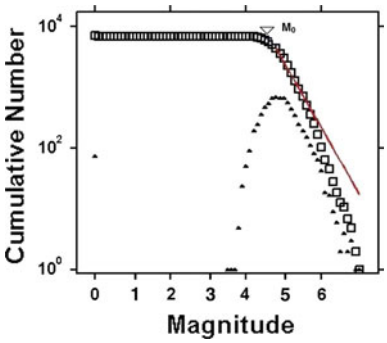

Fig. 3 The relation between cumulative number of events and magnitude indicating the magnitude ($Mo = 4.5$) of completeness

This exercise generated 312 grids. Fractal correlation dimension (D_2) and the frequency-magnitude relation b-value are estimated using the epicentres in the grids, each containing more than or equal to 50 events; other grids are discarded. Centre of each grid is taken as the plotting point for making contour maps. These results are highlighted that shed new light to understand the seismic characteristics of the active faults along this long subduction zone.

2 Fractal dimension

The most commonly used methods for fractal dimension calculation are the box counting method which measures the capacity dimension D_0 and the correlation integral method which measures the correlation dimension D_2 (Bhattacharya et al. 2002). The correlation dimension D_2 is widely applied in seismology, especially to spatial distribution of epicentres. This technique is preferred to box counting algorithm because of its greater reliability and sensitivity to small changes in clustering properties (Kagan and Knopoff 1980; Hirata 1989). The correlation dimension method measures the spacing between two points, which in this case are the earthquake epicentres (Grassberger and Procaccia 1983).

The fractal dimension of the spatial distribution of seismicity is calculated from the correlation integral relation given by Grassberger and Procaccia (1983):

$$D_{\mathrm{wr}} = \lim_{r \to 0} \log(C_r)/\log r \tag{1}$$

where (C_r) is the correlation function.

$$C(r) = \frac{1}{N(N-1)} N_{(R<r)} \tag{2}$$

where $N_{(R<r)}$ is the number of pairs (X_i, X_j) with a smaller distance than r. If the epicentre distribution has a fractal structure, we obtain the following relation:

$$C(r) \sim r^{D_2} \tag{3}$$

where D_2 is a fractal dimension, more strictly, the correlation dimension (Grassberger and Procaccia 1983). By plotting $C(r)$ against r on a double logarithmic coordinate, we can practically obtain the fractal dimension D_2 from the slop of the graph. The distance (r) between two events, (θ_1, ϕ_1) and (θ_2, ϕ_2), is calculated by using a spherical triangle as given by Hirata (1989):

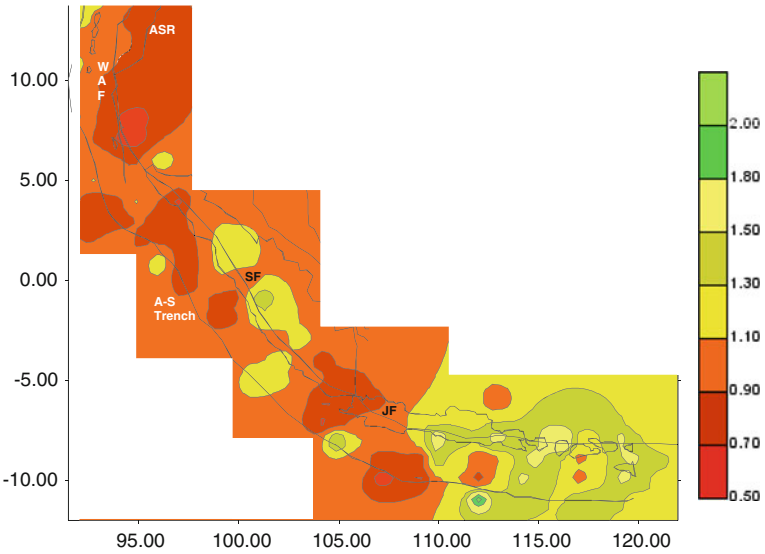

Fig. 4 Contours of fractal dimension of the study region

$$r = \cos^{-1}(\cos\theta_1\cos\theta_2 + \sin\theta_1\sin\theta_2\cos\,(\phi_1 - \phi_2)) \tag{4}$$

The slope is obtained by fitting a least-square line in the scaling region. Using this relation, D_2 (hereafter called Dc) has been calculated, and the map is shown in Fig. 4.

3 Frequency-magnitude relation (*b*-value)

The size of an earthquake is commonly denoted by its magnitude. The statistical distribution of sizes for a group of earthquakes is very complicated. Gutenberg and Richter (1944) provided a simplest frequency-magnitude relation of earthquakes, which describes a power-law relation:

$$\mathrm{Log}_{10}N = a - bM \tag{5}$$

where N is the number of earthquakes in a group having magnitude larger than M, a is a constant, and b is the slope of the log-linear relation. The estimated slope of the log-linear relation or the coefficient b is known as b-value. The b-values are estimated using two methods: least-square fit method and maximum likelihood method. The maximum likelihood method which is based on theoretical consideration is claimed to be a better and stable method (Aki 1965). We have used the maximum likelihood method to estimate the b-value of the earthquakes in selected grids of the region. In this method, the b-value is defined as:

$$b = \frac{\log_{10} e}{\bar{M} - M_o}$$

where $\overline{M}$ is the average magnitude, and Mo is the threshold magnitude. The b-value map is shown in Fig. 5. In addition, five cross sections of b-values across the subduction zone are

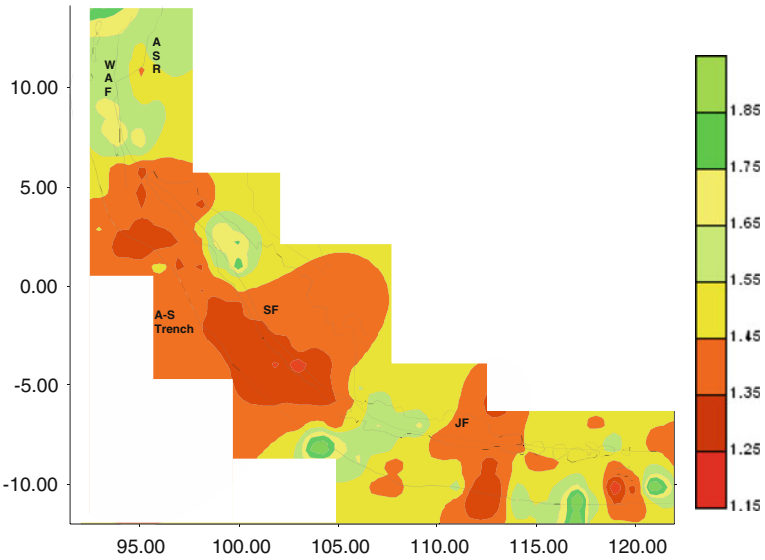

Fig. 5 Contours of *b*-value of the study region

also examined; we have used the Zmap plot (Wiemer and Wyss 1997), and these sections illustrate the variation in *b*-value with depth (Fig. 6).

We have estimated standard deviation δb of the *b*-value using the relation given by Aki (1965) and then the modified formulation given by Shi and Bolt (1982) as follows:

$$\delta b = 2.3b^2 \sqrt{\frac{\sum (M_i - \overline{M})}{n(n-1)}}$$

4 Results and discussion

Tectonic processes generally activate the fault systems in highly stressed zones. Ruptures nucleate from the stressed/asperity zones, which control the distribution of intermediate size and large earthquakes over a fault system. These zones possess different physical states of stress and heterogeneities and hence can be mapped in space and time. Thus, the fractal dimension Dc gives us an estimate of the fractal characteristics of a fault system. A value of Dc close to 3 signifies that the earthquake fractures are filing up a volume of the crust, a value close to 2 suggests that the system is being filled up by a plane, and a value close to 1 means line sources are predominant (Aki 1981). Tosi (1998) illustrated that possible values of fractal dimension of an active fault range between 0 and 2; a set with a Dc close to 0 implies that the epicentres are clustered into one point, and at a value close to 2.0, the epicentres are randomly or homogeneously distributed over a two-dimensional embedding space.

We observe a spatial variation in Dc along the subduction zone from north to south and to south-east, Andaman to Sumatra to Java subduction zones (Fig. 4). At the Andaman-Nicobar subduction zone (Lat 5–15°N), the Dc ranges between 0.7 and 0.9 along the Andaman trench, WAF and ASR. These indicate near linear characteristics of the

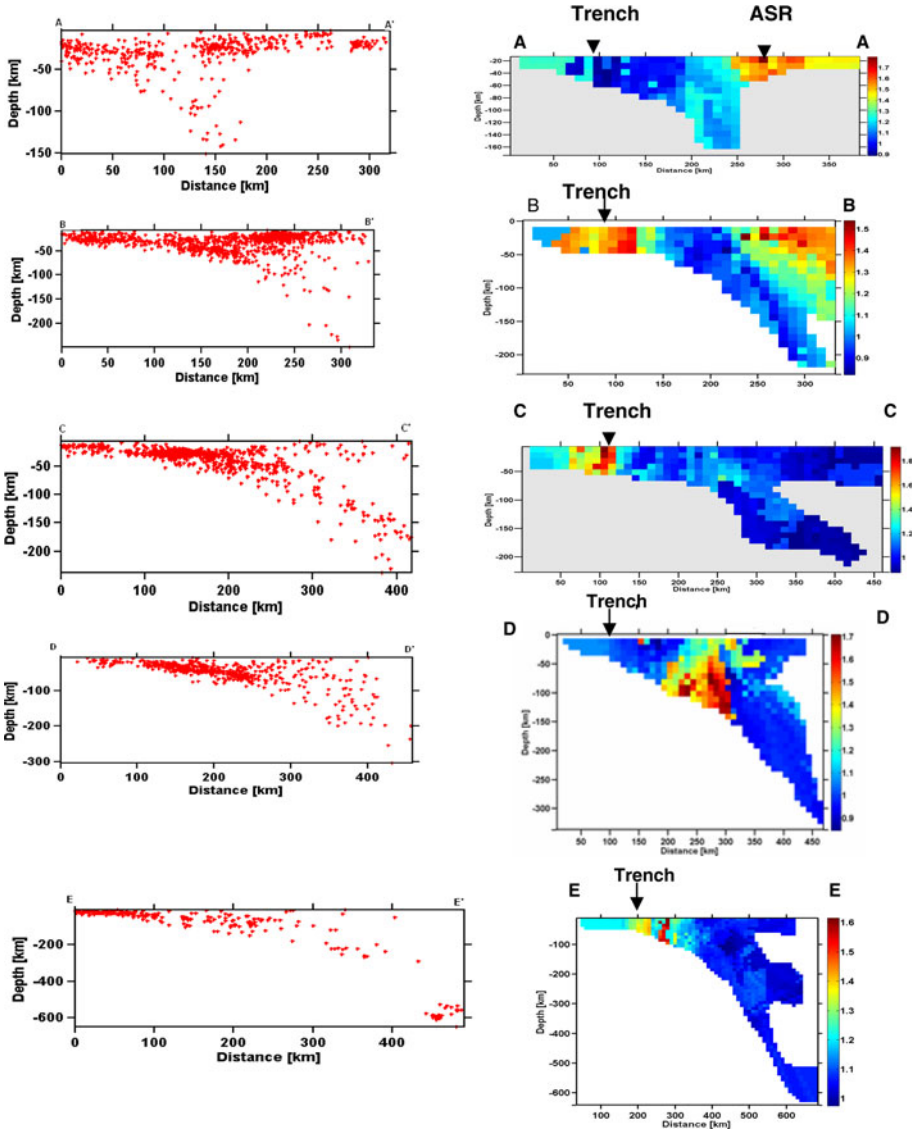

Fig. 6 Depth sections, AA′–EE′ (Fig. 2), showing the Benioff zone and variation of *b*-value

seismogenic structures. At the junction of the WAF and ASR (Lat 6–8°N), the circular contours of the Dc ~ 0.5–0.7, on the other hand, indicate that the epicentres are more in cluster characteristics than linear. Bhattacharya and Kayal (2007) made a fractal study using the lower magnitude ($M > 3.0$) aftershocks occurred during the first 6 months after the 2004 main shock; these were recorded by a local temporary network in the Andaman-Nicobar Islands (Mishra et al. 2007). They reported Dc ~ 1.3 for the WAF, which is higher than our observation Dc ~ 0.7–0.9; both the observations, however, indicate an active linear fault system. The present large data set further revealed a cluster characteristics of the epicentres with a Dc ~ 0.5 at the fault intersection zone of the WAF and ASR

at Lat 6–8°N, which was not identified by the earlier study due to their limited area of study at Lat 9–13°N.

At the Sumatra-Java subduction zone, a similar observation is made; the major structures like the Sumatra-Java trench, the Sumatra and Java fault systems indicate Dc $\sim$ 0.9 to 1.3. In between the major contours of Dc $\sim$ 0.9–1.3, there are several close contour zones with Dc $\sim$ 0.5 to 0.9. These pockets of lower Dc contours are indicative of the epicentre cluster zones along the long subduction zone. The findings are much in conformity with active fault/subduction zones, similar to that (Dc $\sim$ 0.5 to 1.5) made by Shimazaki and Nagahama (1995) in the Japan subduction zone and by Angulo-Brown et al. (1998) in the Mexican subduction zone. The areas of cluster characteristics with Dc $\sim$ 0.5 to 0.9 within the long linear Sumatra-Java fault systems possibly indicate the highly stressed zones, the zones of asperity, that accumulate more stress for rupture nucleation of intermediate to large earthquakes.

The frequency-magnitude relation, *b*-value, is an important seismological parameter that may be related to structural heterogeneity, crack density, thermal gradient, depth and stress distribution (Mogi 1962; Scholz 1968; Wyss 1973; Urbancic et al. 1992; Wiemer et al. 1998). Although an average *b*-value is $\sim$1.0 in an active zone, it may vary from 0.5 to 2.0 depending on the tectonic regime (Wiemer and Wyss 1997; Nanjo et al. 1998). In shield area, the *b*-value is much less (0.4–0.5) (Kayal 2000), whereas in seismically active region, it is between 1.0 and 1.5, and for volcanic activity or swarm activity it may go up to 2.0 (Wiemer and McNutt 1997; Kayal 2008).

In this study, the *b*-value map broadly illustrates the variation between 1.15 and 1.55 (Fig. 5), which is mostly observed in a seismically active tectonic zone. The WAF–ASR zone is reflected with a *b*-value 1.5; it implies the higher frequency of lower magnitude events in this zone compared with the zones to its south. Great earthquakes in such zone are more unlikely. It is, however, interesting to note that the northern and southern ends of the WAF–ASR zone are reflected with the close contours of $b \sim 1.4$–1.5. The higher $b \sim 1.5$ contour zone at the northern end below Lat 15°N may indicate the region of a strong earthquake Mw 6.5 in 13 September 2002 with a NW–SE trending aftershock zone (Kayal et al. 2004). Kayal et al. (2004) interpreted this NW–SE trending main shock and aftershock source zone as a transverse seismic structure to the N–S trending Andaman trench. No much seismic activity is observed to the north of this structure, at Lat 15–18°N, whereas intense activity is observed farther north at the Indo-Burma subduction zone (Kayal 2008). The rupture propagation of the 2004 mega thrust earthquake stopped at this NW–SE transverse structure below the Lat 15°N. Aseismicity to the north of this transverse structure at Lat 15–18°N is explained by thick sediments of the Irrawady basin (Kayal 2008). Recently, Kundu and Gahalaut (2010), however, postulated tearing and thinning of the Indian subducting slab to explain the aseismicity at 15–18°N. The close contour with *b*-value 1.4 is prominent at the southern end, at the intersection zone of the WAF and the ASR. This fault intersection zone is also identified by lower fractal dimension Dc 0.5–0.7, implying it to be a zone of epicentre cluster. To the south, the entire Sumatra-Java subduction zone is mapped with $b \sim 1.15$ to 1.5, and a few pocket areas show lower $b > 1.3$. These pocket areas of lower *b*-values are indicative of comparatively more stressed zone or zone of asperity, and these are also identified as cluster zone of epicentres with lower Dc $\sim$ 0.5 to 0.7. Thus, a positive correlation between *b*-value and Dc is observed in the Andaman-Sumatra-Java subduction zone. The standard error of *b*-value, δb, calculated for this region varies between $\pm$0.01–0.18.

Five cross sections of the *b*-values with depth are examined along A–A′ to E–E′, almost across the subduction zone along the Andaman-Sumatra-Java trench (Fig. 6). These

sections depict the Benioff zone or subducted seismic slab and the changes in *b*-values in the different tectonic structures with depth. The section A–A′ at Lat 15°N shows that at the trench and along the Benioff zone, the *b*-value is 0.8–1.3, and at the ASR, the value goes up to 1.5. This implies the tectonic stress is more at the subduction zone than at the ASR. The section B–B′ at Lat 8°N, across the WAF and ASR intersection, on the other hand, shows slightly higher *b*-value 1.3 at the trench and comparatively lower or normal *b*-value 1.0 at the WAF–ASR intersection. This signifies higher frequency of lower magnitude earthquakes at the trench, whereas the fault intersection zone accumulates more stress and follows the normal frequency-magnitude relation. The earthquakes in the Benioff zone in this section, however, look diffused. The section C–C′ at Lat 0° shows a more defined Benioff zone down to 150 km with near normal *b*-values 1.0–1.2, and with higher *b*-values 1.3–1.5 at the trench. The overriding plate also shows near normal *b*-value 1.0–1.2. This implies higher tectonic stress in the subducting as well as in the overriding plate compared to the trench. The section D–D′ at Lat 5°N illustrates a steep dipping Benioff zone, near the trench with intense activity, and the Benioff zone goes down to 300 km. The trench shows a $b \sim 1.1$, but the shallower part of the subducting slab shows comparatively much lower or near normal $b \sim 0.9$ to 1.0, and the deeper part of the subducting plate as well as the overriding plate shows lower *b*-value ~ 0.9. In between shallower part and the deeper part, there is a zone of higher *b*-value ~ 1.3 to 1.5. This observation clearly depicts that the upper part of the subducting slab is under more stress due to bending of the plate compared with its lower part, which is the intermediate part, and the deeper part of the slab is again under higher stress. The section E–E′ is nearly N–S across the Java trench, and it shows a much deeper Benioff zone, down to 650 km. The trench is reflected with a higher $b \sim 1.3$ to 1.4, but the subducting zone is defined with near normal $b \sim 1.0$ to 1.1. It is interesting to note a less seismic activity at 350–450 km depth within the Benioff zone along the Java trench.

5 Conclusions

About 8,000 earthquakes at the Andaman-Sumatra subduction zone, recorded during 1964–2007, located by the EHB method, have been very useful to map fractal correlation dimension (Dc) and frequency-magnitude relation (*b*-value). The Dc and *b*-value characteristics of the tectonic structures/active faults along this ~3,000-km-long subduction zone shed new light in our understanding of subduction zone earthquake characteristics. The trench zones show higher Dc ~ 1.0 to 1.4 and higher $b \sim 1.2$ to 1.4 implying linear structure and more frequency of lower magnitude earthquakes. The trench parallel active fault systems in the fore-arc zone show lower Dc 0.8–1.0 and near normal $b \sim 1.0$ to 1.2. These observations indicate that the trench parallel active faults in the fore arc are more linear and possess near normal frequency-magnitude relation. Several pocket zones of lowest Dc 0.4–0.6 and lowest *b*-value 0.8–1.0 *b* along these long fault systems are inferred to be the more stressed zones or asperity zones, where intermediate to strong earthquakes nucleate. The WAF–ASR in the Andaman Sea shows higher $b \sim 1.4$, possibly indicating lesser tectonic stress compared to the fore-arc fault systems. The depth sections illustrate depth variations in *b*-value of the seismogenic structures/active faults. The trench zones and the ASR show higher b with depth. The Benioff zone shows lower b at the upper part of the subducting slab where tectonic stress is more due to bending. The lower part of the subducting slab shows higher b across the Sumatra subduction zone compared with other deeper part in the Java subduction zone. The observed Dc and *b*-values give us a better

understanding of the seismic characteristics of different seismogenic structures along this long subduction zone and are useful to risk evaluation in its different segments.

Acknowledgments All earthquakes were located by the EHB method (Engdahl et al. 2008), and listing of the events were available from E. R. Engdahl (Personal Communication 2009). The Zmap software (Wiemer et al. 2001) version is used for the *b*-value depth sections. The Council of Scientific and Industrial Research (CSIR), Government of India, New Delhi, sponsored the research project.

References

Aki K (1965) Maximum likelihood estimation of b in the formula log N = a–bM and its confidence limits. Bull Earthquake Res Inst Tokyo Univ 43:237–239

Aki K (1981) Earthquake prediction, vol 4. Am Geophys Union, Washington, pp 566–574

Angulo-Brown F, Ramirez-Guzman AH, Tepez E, Rudoif-Navarroa A, Pavia-Miller CG (1998) Fractal geometry and seismicity in the Mexican subduction zone. Geofisica Int 37:29–33

Bhattacharya PM, Kayal JR (2007) Application of fractal in marine sciences: study of the 2004 Sumatra earthquake (Mw 93) sequence in Andaman-Nicobar Islands. Indian J Mar Sci 36(2):136–140

Bhattacharya PM, Majumdar RK, Kayal JR (2002) Fractal dimension and b-value mapping in northeast India. Curr Sci 82(12):1486–1491

Bilham R (2005) A flying start then a slow slip. Science 308:1126–1127

Curray JR (2005) Tectonics and history of the Andaman Sea region. J Asian Earth Sci 25:131–140

Curray JR, Moore DG, Lawver LA, Emmel FJ, Raitt RW, Henry M, Kieckhefer R (1979) Tectonics of the Andaman Sea and Burma. In: Watkins JS, Montadert L, Dickenson P (eds) Geological and geophysical investigations of continental margins. Am Asoc Pet Geol Mem, pp 189–198

DeMets C, Gordan RG, Argus DF, Stein S (1994) Effect of recent revisions to the geomagnetic reversal time scale on estimates of current plate motions. Geophys Res Lett 21:2191–2194

Dimri VP (2000) Fractal behaviour of the earth system. Springer, Berlin

Engdahl ER, Villasenor A, Deshon HR, Thurber CH (2007) Teleseismic relocation and assessment of seismicity (1918–2005) in the region of the 2004 M_w Sumatra-Andaman and 2005 M_w 8.6 Nias Island Great Earthquakes. Bull Seism Soc Am 97(1A):s43–s61

Fitch TJ (1970) Earthquake mechanisms in the Himalaya Burmese and Andaman regions and continental tectonics in Central Asia. J Geophys Res 75:2699–2709

Grassberger P, Procaccia I (1983) Measuring the strangeness of strange attractors. Physica D 9:189–208

Gutenberg R, Richter CF (1944) Frequency of earthquakes in California. Bull Seism Soc Am 34:185–188

Hirata T (1989) A correlation between the b-value and fractal dimension of earthquakes. Jour Geophys Res 94:7507–7514

Kagan YY, Knopoff L (1980) Spatial distribution of earthquakes: the two point correlation function. Geophys J R Astron Soc 62:303–320

Kayal JR (2000) Seismotectonic study of the two recent earthquakes in Central India. J Geol Soc India 55:123–138

Kayal JR (2008) Microearthquake seismology and seismotectonics of South Asia. Springer, The Netherlands

Kayal JR, Gaonkar SG, Chakraborty GK, Singh OP (2004) Aftershocks and seismotectonic implications of the 13th September 2002 earthquake (M_w 65) in the Andaman Sea Basin. Bull Seism Soc Am 94(1):326–333

Kundu B, Gahalaut K (2010) An investigation into the seismic potential of the Irrawady Region Northern Sunda Arc. Bull Seism Soc Am 100(2):891–895 (short note)

Mandelbrot BB (1982) The fractal geometry of nature. Freeman, Sanfrancisco

Mishra OP, Kayal JR, Chakraborty GK, Singh OP, Ghosh D (2007) Aftershock investigation in the Andaman Nicobar islands of India and its seismotectonic implications. Bull Seism Soc Am 97(1A): S71–S85

Mogi K (1962) Magnitude-frequency relation for elastic shocks accompanying fractures of various materials and some related problems in earthquakes. Bull Earthquakes Res Inst Uni Tokyo 40:831–853

Mogi K (1967) Earthquakes and fractures. Tectonophysics 5(1):35–55

Mori J, Abercrombi RE (1997) Depth dependence of earthquake frequency-magnitude distribution in California: implications for the rupture initiation. J Geophys Res 102:15081–15090

Nanjo K, Nagahma H, Satomura M (1998) Rates of aftershock decay and the fractal structure of active fault systems. Tectonophysics 287:173–186

Ogata Y (1988) Statistical models for earthquake occurrences. J Am Stat As 83(401):9–27
Scholz CH (1968) The frequency-magnitude relation of microfracturing in rocks and its relation to earthquakes. Bull Seism Soc Am 58:399–415
Seih K, Natawidjaja D (2000) Neotectonics of Sumatran fault, Indonesia. J Geophys Res 105(B): 28295–28326
Shi Y, Bolt B (1982) The standard error of magnitude-frequency b value. Bull Seism Soc Am 72:1677–1687
Shimazaki T, Nagahama H (1995) Do earthquakes occur at random collectivities and individualities of earthquakes. Kagaku (Science Iwanami shotten Tokyo 65:241–256 (in Japanese)
Sunmonu A, Dimri VP (1999) Fractal analysis and seismicity of Bengal basin and Tripura fold belt, northeast India. J Geol Soc India 53:587–592
Teotia SS, Kumar D (2007) The Great Sumatra-Andaman earthquake of 26 December 2004 was predictable even from seismicity data of mb $>$ 4.5: a lesson to learn from nature. Indian J Mar Sci 36(2):122–127
Tosi P (1998) Seismogenic structure behaviour revealed by spatial clustering of seismicity in the Umbria-Marche Region (Central Italy). Annali Di Geofisica 41(2):215–224
Urbancic TI, Trifu CI, Long JM, Young RP (1992) Space-Time correlations of b-values with stress release. Pure Appl Geophys 139:449–462
Wang Z, Lu H (1997) Evidence and dynamics for the change of the strike-slip direction of the Changle-Nannao Ductile shear zone South East China. J Asian Earth Sci 15(6):507–515
Wiemer S, McNutt SR (1997) Variations I the frequency magnitude distribution with depth in two volcanic areas: Mount St. Helens, Washington, Mount Spurr Alaska. Geophys Res Let 24(2):189–192
Wiemer S, Wyss M (1997) Mapping the frequency-magnitude distribution in asperities: an improved technique to calculate recurrence times. J Geophys Res 102:15115–15128
Wiemer S, Mcnutt SR, Wyss M (1998) Temporal and three dimensional spatial analysis of the frequency-magnitude distribution near Long Valley Caldera, California. Geo phys J Int 134:409–421
Wyss M (1973) Towards a physical understanding of the earthquake frequency distribution. Geophys J R Astron Soc 31:341–359
Wyss M, Klein F, Nagamine K, Weimer S (2001) Anomalously high b-values in the South Flank of Kilauea Hawaii: evidence for the distribution of magma below Kilauea's East Rift Zone. J volcanol Geotherm Res 106:23–37